

Comparative High Field Magneto-Transport of Rare Earth Oxypnictides with Maximum Transition Temperatures

J. Jaroszynski, Scott C. Riggs, F. Hunte, A. Gurevich, D. C. Larbalestier, and G. S. Boebinger
National High Magnetic Field Laboratory, Florida State University, Tallahassee, FL, 32310

F. F. Balakirev and Albert Migliori
National High Magnetic Field Laboratory, Los Alamos National Laboratory, Los Alamos, NM, 87545

Z. A. Ren, W. Lu, J. Yang, X. L. Shen, X. L. Dong, Z. X. Zhao
National Laboratory for Superconductivity, Institute of Physics and Beijing National Laboratory for Condensed Matter Physics,
Chinese Academy of Sciences, P. O. Box 603, Beijing 100190, P. R. China

R. Jin, A. S. Sefat, M. A. McGuire, B. C. Sales, D. K. Christen, and D. Mandrus
Materials Science Division, Oak Ridge National Laboratory, P. O. Box 2008, Oak Ridge, TN 37831
(dated: February 20, 2024)

We compare magneto-transport of the three iron-arsenide-based compounds ReFeAsO ($\text{Re} = \text{La}, \text{Sm}, \text{Nd}$) in very high DC and pulsed magnetic fields up to 45 T and 54 T, respectively. Each sample studied exhibits a superconducting transition temperature near the maximum reported to date for that particular compound. While high magnetic fields do not suppress the superconducting state appreciably, the resistivity, Hall coefficient and critical magnetic fields, taken together, suggest that the phenomenology and superconducting parameters of the oxypnictide superconductors bridges the gap between MgB_2 and YBCO .

PACS numbers: 74.70.-b, 74.25.Fy, 74.72.-h, 74.81.Bd

The recently discovered layered superconducting oxypnictides with high transition temperatures [1] are based on alternating structures of FeAs and ReO layers. Similar to the high-temperature superconducting cuprates, superconductivity in oxypnictides seem to emerge upon doping of a parent antiferromagnetic state. As the ReO planes are doped, the ionically bonded ReO donates an electron to the covalently bonded FeAs plane [2], suppressing the global antiferromagnetism and resulting in superconductivity. Different rare earths do, however, have an effect on the superconducting transition temperature, T_c , which, increases from a maximum of 28 K for La [2, 3] to above 40 K for Ce [4] and above 50 K for Nd, Pr, Sm and Gd, respectively [5, 6, 7, 8]. Unlike the cuprates, the doping required for the onset of superconductivity, as well as the doping at optimal T_c , seems to depend on the specific rare earth in the compound, perhaps for intrinsic reasons such as a varying the magnetic moment or size of the rare earth atom, or a possible role of multiple bands.

To deduce common behaviors of the oxypnictide superconductors, we studied three of the iron-arsenide-based compounds ReFeAsO ($\text{Re} = \text{La}, \text{Sm}, \text{Nd}$) in very high magnetic fields. All samples measured were polycrystals made by solid state synthesis. Two were doped by partial F substitution for O (La and Nd) and one (Sm) by forcing an O deficiency. The $\text{SmFeAsO}_{0.85}$ [9] and $\text{NdFeAsO}_{0.94}\text{F}_{0.06}$ [5], exhibiting a 90 % $T_c = 53.5$ K and 50.5 K, respectively, were grown at the National Laboratory for Superconductivity in Beijing. These sam-

ples result from high-pressure synthesis. SmAs (or NdAs) pre-sintered powder and Fe , Fe_2O_3 , and FeF_2 powders were mixed together according to the nominal stoichiometric ratio then ground thoroughly and pressed into small pellets. The pellets were sealed in boron nitride crucibles and sintered in a high pressure synthesis apparatus under a pressure of 6 GPa at 1250 °C for 2 hours. The $\text{LaFeAsO}_{0.89}\text{F}_{0.11}$ sample from the Oak Ridge group has $T_c = 28$ K [3], which is among the highest transition temperatures reported for this compound at ambient pressure [2]. It was grown by a standard solid-state synthesis method similar to that reported previously [1], from elements and binaries, with purity > 4 N. Our extensive studies on morphology, connectivity, electromagnetic granularity, phase purity, magnetic properties etc. could be found elsewhere [10, 11, 12].

Phase diagrams for fluorine-doping [1, 13, 14] have been reported for each compound: our $\text{LaFeAsO}_{0.89}\text{F}_{0.11}$ and $\text{SmFeAsO}_{0.85}$ samples are deemed optimally doped based upon the maximal value of T_c in the published F-doped phase diagrams, which is consistent with the nominal F-doping level for our samples [1, 13, 14]. It is important to note, however, that the actual doping of polycrystalline samples can be difficult to determine precisely. For example, the nominal doping of $x = 0.06$ in our $\text{NdFeAsO}_{0.94}\text{F}_{0.06}$ sample is anomalously low in light of the published phase diagram, for which an experimental value of $T_c = 50.5$ K corresponds to the maximum value of T_c , which is reported to occur at an F-doping of around 11 %. However, in contrast to the cuprates,

the optimal doping range for these superconductors is wide. On the other hand, from technological point of view, it is often that the real F-content is much smaller than the nominal for the ambient-pressure sintered samples, since lots of F was observed to react with quartz glass. However, we observe rather higher than nominal doping, probably because our Nd sample was high pressure sintered. This method has a better doping effect, in contrast to ambient pressure samples which were used for the construction of the phase diagram [14]. Despite the uncertainty in doping levels, we believe that all three of our samples are near optimal doping, because they exhibit transition temperatures very near the consensus values of highest T_c for these compounds at ambient pressure.

The longitudinal resistivity ρ_{xx} and the Hall coefficient R_H in high magnetic fields were measured using a lock-in technique in three different high-field magnets at the National High Magnetic Field Laboratory (NHMFL): 33 T DC resistive and 45 T hybrid magnets at Florida State University, and 54 T pulsed magnets at Los Alamos National Laboratory. For each experiment, the samples were nominally rectangular prisms and the magnetic field was applied perpendicular to the largest face of the samples. Six electrical contacts (using either DuPont silver paint or Epo-tek H20 E silver epoxy) were positioned around the perimeter of the sample in a conventional Hall bar geometry.

Figure 1 a shows ρ_{xx} as a function of temperature T at $B = 0$ for the $\text{LaFeAsO}_{0.89}\text{F}_{0.11}$, $\text{SmFeAsO}_{0.85}$, and $\text{NdFeAsO}_{0.94}\text{F}_{0.06}$ samples. $\text{LaFeAsO}_{0.89}\text{F}_{0.11}$ exhibits a conventional super-linear T -dependence of $\rho_{xx}(T)$. A magnetic field suppresses superconductivity by shifting the resistive transition to lower T , reducing T_c by roughly a factor of two with 30 T, as shown in Fig. 1 b.

$\text{SmFeAsO}_{0.85}$ and $\text{NdFeAsO}_{0.94}\text{F}_{0.06}$ show strikingly different behavior that is more reminiscent of the high-temperature superconducting cuprates: a linear temperature dependence of $\rho_{xx}(T)$, from 225 K down to T_c and a substantial broadening of the resistive transition in a magnetic field: applying 33 T has little effect on the high-temperature superconductivity onset, while the foot of the transition is shifted to substantially lower temperature as shown in Fig. 1 c and d.

The field dependencies of the Hall resistivity ρ_{xy} are shown in Fig. 2 a,b, and c for the La, Sm, and Nd compounds, respectively, over a wide temperature range above T_c . The low temperature behavior of the La compound at $T < 100$ K in Fig. 2 a is rather conventional: ρ_{xy} is linear in B and is temperature independent. If only one band contributes to current transport, the Hall coefficient, $R_H = \rho_{xy}/B = 1/ne$, yields a carrier density n of 0.07 electrons per unit formula in the La compound at low temperatures. Here we used reported unit cell parameters [15] with two unit formulas per unit cell. This value is not far from the nominal doping of $x = 0.1$ per

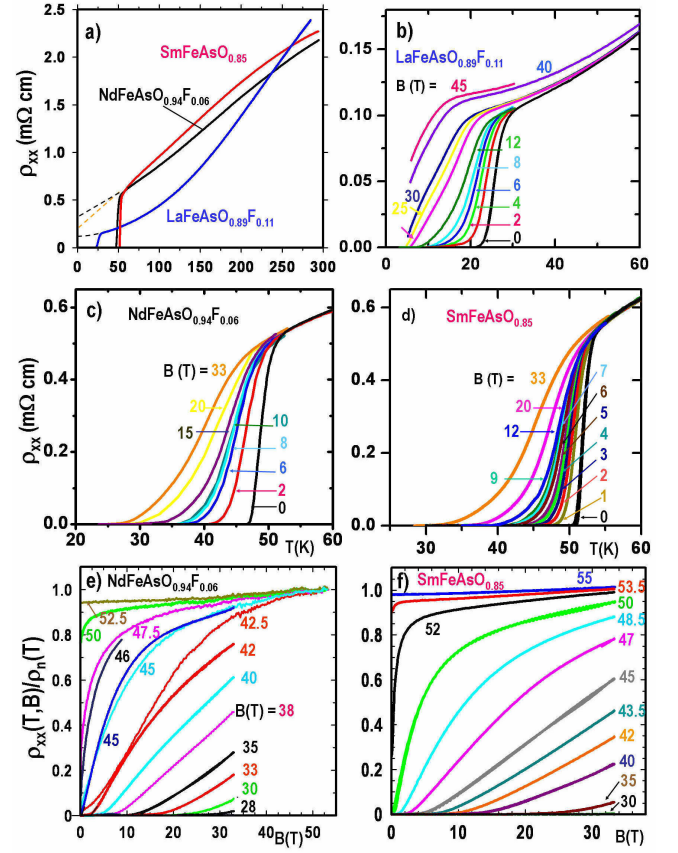


FIG. 1: (a) Longitudinal resistivity $\rho_{xx}(T)$ at $B = 0$ for three members of the $\text{ReO}_{1-x}\text{F}_x\text{FeAs}$ system: $\text{LaFeAsO}_{0.89}\text{F}_{0.11}$ with $T_c \sim 28$ K, $\text{SmFeAsO}_{0.85}$ with $T_c \sim 53.5$ K, and $\text{NdFeAsO}_{0.94}\text{F}_{0.06}$ with $T_c \sim 50.5$ K. Dashed lines show normal resistance $\rho_n(T)$ extrapolated below T_c . (b) ρ_{xx} at various magnetic fields as a function of temperature for La compound at $B = 0, 2, 4, 6, 8, 12, 20, 25, 30, 40$ and 45 T; (c) Nd compound at $B = 0, 2, 6, 8, 10, 15, 20$, and 33 T; and (d) for Sm compound at $B = 0, 1, 2, 3, 4, 5, 6, 7, 8, 9, 12, 25$ and 33 T. (e) Normalized resistivity $\rho_{xx}(T,B)/\rho_n(T)$ of Nd sample vs. B at various T measured in DC resistive magnet up to 33 T (sweep rate 5 T/min) and pulsed magnetic field up to 54 T. The latter data exhibit saturation at lower temperatures which may result from eddy current heating in this relatively big sample. (f) $\rho_{xx}(T,B)/\rho_n(T)$ of Sm sample versus B at various T measured in DC resistive magnet up to 33 T.

unit formula.

At higher T all three compounds exhibit a strong temperature dependence of ρ_{xy} as is evident in Figs. 2 a,b, and c. Note however that all traces in Fig. 2 retain a linear dependence on B regardless of temperatures. The observed strictly linear field dependence of ρ_{xy} and no magnetoresistance at temperatures 70 – 200 K indicates that $\omega_c \ll 1/\tau$, where $\omega_c = eB/m$ is the cyclotron frequency and τ is the scattering time. At the same time the observed temperature dependence of R_H may indicate two-band effects.

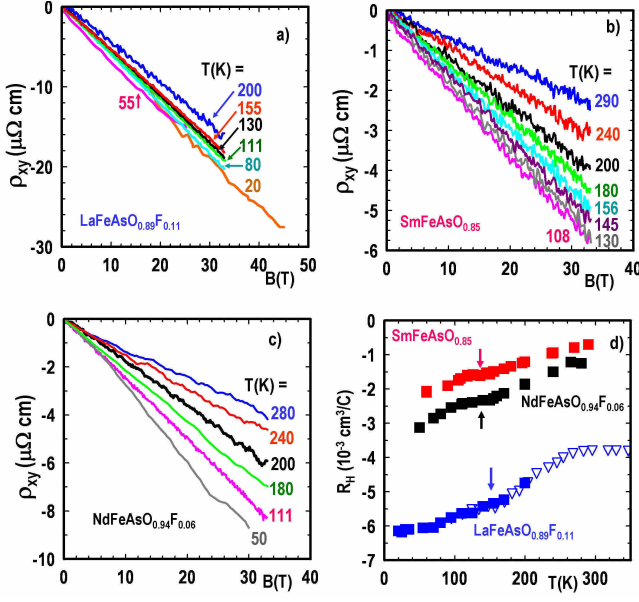


FIG. 2: The Hall resistivity ρ_{xy} versus magnetic field for: (a) La-compound, (b) Sm-compound and (c) Nd-compound at $T > T_c$. Note that all ρ_{xy} show a linear dependence on magnetic field. The low-temperature ρ_{xy} for the La compound are also temperature independent, consistent with a dominant single-carrier conduction mechanism, while at higher T all compounds show marked $\rho_{xy}(T)$ dependencies. (d) Hall coefficient determined from linear fits to $\rho_{xy}(H)$ for $33 < B < 33 \text{ T}$ or $11.5 < B < 45 \text{ T}$ (solid squares) and at $B = 9 \text{ T}$ (open triangles Ref. [3]). No systematic departure from linearity was found regardless of temperature. Arrows show apparent inflections on $R_H(T)$ dependence around $T \approx 150 \text{ K}$, which may result from structural transitions.

A number of experimental [16, 17, 18] and theoretical [19, 20, 21] papers have discussed the oxypnictides as a two-band system. In this case, the primary effect of high magnetic fields is the lateral separation of electron-like and hole-like carriers. Often ρ_{xy} for a semimetal is not a linear function of H due to the complexity of the transport in the presence of two different carriers. The field dependence of R_H for a two band system [22]

$$R_H = \frac{\frac{1}{2}R_1 + \frac{1}{2}R_2 + \frac{1}{2}\frac{1}{2}R_1R_2(R_1 + R_2)B^2}{(\frac{1}{2} + \frac{1}{2})^2 + \frac{1}{2}\frac{1}{2}(R_1 + R_2)^2B^2} \quad (1)$$

becomes noticeable as the parameter $\beta_c = B/B_0$ becomes of the order of unity provided that $R_1 \neq R_2$ and $\frac{1}{2} \neq \frac{1}{2}$. Here $B_0 = \frac{1}{2}R_1R_2$, the indices 1 and 2 correspond to bands 1 and 2, $R_{1/2}$ and $\frac{1}{2} = \frac{1}{2}$ are intraband Hall coefficients and conductivities, respectively, and ρ_{xx} is determined by the minimum value of $\frac{1}{2}$ and $\frac{1}{2}$ in the parallel band connection. Taking the characteristic values of $\rho_{xx} \approx 1 \text{ m}\Omega \text{ cm}$ and $R_H \approx 5 \times 10^{-3} \text{ cm}^3/\text{C}$ from Figs. 1 and 2, we get $B_0 = 2000 \text{ T}$, indicating that $\beta_c \gg 1$ only at inaccessible magnetic fields $H > 1000 \text{ T}$. The same field B_0 sets the scale for the onset of magnetoresistance. Note that in Fig. 1, there is no

significant magneto-resistance above T_c , where the zero field data (black line) superimpose data taken in magnetic fields. Thus, the observed temperature dependence of R_H is consistent with a two-band system at $\beta_c \approx 1$ for both bands with no visible magnetoresistance and the Hall resistivity $\rho_{xy} = B(\frac{1}{2}R_1 + \frac{1}{2}R_2) = (\frac{1}{2} + \frac{1}{2})^2$ linear in B .

Figure 2d shows the marked temperature dependencies of R_H , which exhibit pronounced inflections at temperatures marked by the three arrows. These arrows indicate the temperatures at which a structural phase transition has been reported for the three undoped parent compounds. Neutron data on undoped LaFeAsO show a transition from tetragonal to monoclinic lattice around 150 K , followed by antiferromagnetic ordering below 134 K [23]. SmFeAsO shows a tetragonal to orthorhombic transition at 129 K [24]. For NdFeAsO , sharp jumps in heat capacity signal structural transition at 150 K [25]. Unlike the pseudogap in the cuprates, doping of the parent compound only slightly reduces the temperature of these anomalies in the oxypnictides as the doping approaches the range in which superconductivity is observed [1, 13, 14]. The Hall data in Fig. 2 suggest that a remnant of the structural transitions in the undoped parent compounds manifest themselves at optimum doping as well, however it is also possible, that this results from the presence of undoped phase in the samples. At the same time the overall temperature dependence of $R_H(T)$ is not understood.

Finally, the high-field longitudinal resistivity measurements shown in Fig. 1 enable a characterization of the magnetic field scales required to suppress superconductivity in the oxypnictides. Figure 3 shows three characteristic fields $H_{90}(T)$, $H_{50}(T)$ and $H_{10}(T)$ at which $\rho_{xx}(T)$ reaches 90%, 50% and 10% of the normal state resistivity $\rho_n(T)$ extrapolated linearly from its temperature dependence above T_c . For all three compounds, the data in Fig. 3 are reminiscent of the quasi-2D layered cuprate superconductors [26]. Following a previous analysis for polycrystalline samples [16], we assume that, because of the strong angular dependence of $H_{c2}(\theta)$, the field $H_{10}(T)$ scales like H_{c2}^2 parallel to the c -axis, that is, the geometry for which the magnetic field most readily suppresses the superconducting state. The resistivity $\rho_{xx}(T;H)$ at the very bottom of the transition, say at 0.5% ρ_n matches the onset of the pinned critical state of vortices below the irreversibility field $H_{irr}(T)$ extracted from magnetization measurements [10]. The 90% data in turn likely corresponds to $H_{c2}(T)$ perpendicular to the c -axis, as only at this point has superconductivity been largely suppressed for all orientations of the polycrystalline grains.

Shown in Fig. 3b are the magnetic fields $H_{90}(T)$, $H_{50}(T)$ and $H_{10}(T)$ normalized to the respective values of T_c^2 for each compound and plotted as functions of the reduced temperature $t = T/T_c$. All $H_{50}(T)$ and

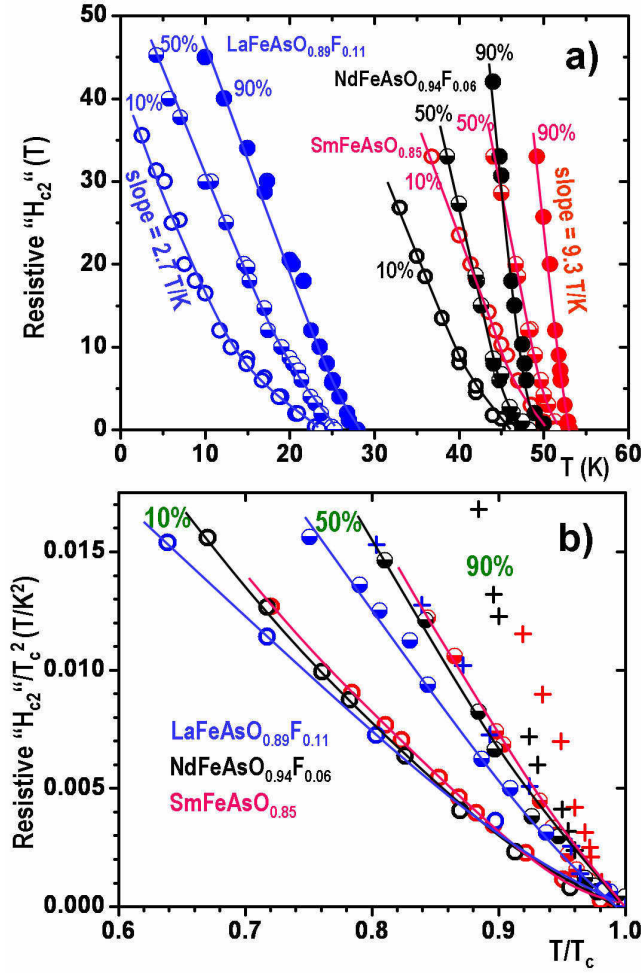


FIG. 3: (a) Upper critical fields H_{c2} versus temperature for the Sm-, Nd- and La-compounds. with $T_c = 53.5$ K, 50.5 K, and 28 K respectively, as determined from 90 % transitions; $T_c = 52$ K, 47.5 K, and 25 K for 50 % transitions and $T_c = 51$ K, 46 K, and 23 K for 10 % transitions. The data extracted from the results shown in Fig. 1, show the temperatures at which the resistance reaches 10 %, 50 % and 90 % of the normal state resistance, as extrapolated linearly from the $n(T)$ temperature dependence above T_c . The solid lines guide the eye. (b) The same data divided by T_c^2 and plotted as a function of reduced temperature T/T_c .

$H_{10}(T)$ data nearly collapse onto single curves, while the $H_{90}(T)$ data do not. This behavior suggests the following qualitative interpretation. The upper critical fields $H_{c2}^k = 2 \frac{\hbar^2}{4\pi m_a c} \frac{1}{a}$ along the c -axis and perpendicular to the c -axis, $H_{c2}^k = 2 \frac{\hbar^2}{4\pi m_a c} \frac{1}{a}$ are defined by the respective coherence lengths, ξ_a and ξ_c , $\xi_c = \xi_a \frac{1}{\gamma}$, where $\gamma = \frac{m_c}{m_a}$ is the effective mass or resistivity anisotropy parameter. Given the nanoscale ξ_a and ξ_c in oxypnictides [16], we can assume that these materials even in the present polycrystalline form are likely in the clean limit, $\xi_a < \lambda$, where λ is the mean free path. In this case $\xi_a / \xi_c = 1/T_c$, which yields H_{c2} / T_c^2 , consistent with the scaling of $H_{50}(T)$ and $H_{10}(T)$ curves defined by H_{c2}^2 in Fig. 4b for all three

compounds. In turn, the lack of scaling for $H_{90}(T)$ defined by $H_{c2}^k(T)$ in Fig. 3b may indicate that, in addition to the change in T_c , the mass anisotropy parameter also changes, as will be discussed below.

Our high-field data enable us to make several further conclusions regarding trends in superconducting oxypnictides. From the measured $R_H = 1/ne$ and the London penetration depth $\lambda_0^2 = m_0/ne^2$ at $T = 0$, we estimate the effective mass of the carriers $m = m_0 \frac{\lambda_0^2}{R_H}$, where e is the electron charge. Taking $R_H = 62 \times 10^{-3} \text{ cm}^3/\text{C}$ at T_c from Figs. 1 and 2 and $\lambda_0 = 215$ nm from NMR data [27], we obtain $m = 1.6m_e$ for $\text{LaFeAsO}_x\text{F}_{1-x}$ (or a slightly higher $m = 2.23m_e$ for $\lambda_0 = 254$ nm taken from SR data [28]). For SmFeAsO , we take $R_H = 2 \times 10^{-9} \text{ m}^3/\text{C}$ from Figure 2 and $\lambda_0 = 184$ nm from SR data [29], which yields $m = 3.7m_e$. The increase of m^* as T_c increases from 28 K for $\text{LaFeAsO}_x\text{F}_{1-x}$ to 53.5 K for SmFeAsO may reflect the effective mass renormalization by strong coupling effects [30]. The above one-band estimate can also be applied qualitatively to two-band systems, in which either the ratios $m_1 = n_1$ and $m_2 = n_2$ are not too different, or $n_1 \approx n_2$. In the latter case m corresponds to band 1, which effectively short-circuits band 2. In turn, the ratio $n_1 = n_2$ can be controlled by disorder, as has been shown for MgB_2 [31].

The relative effects of vortex fluctuations can be inferred from the data of Fig. 1. As mentioned previously, the $R(T)$ curve for $\text{LaFeAsO}_x\text{F}_{1-x}$ mostly shifts to lower temperatures without much change in shape upon increasing H . This behavior is characteristic of the resistive transition in low- T_c superconductors with weak thermal fluctuations of vortices. By contrast, the $R(T)$ curves for the higher- T_c oxypnictides in Figs. 1c and d broaden significantly as H increases, similar to the behavior of the cuprates. This indicates that thermal fluctuations of vortices in SmFeAsO and $\text{NdFeAsO}_x\text{F}_{1-x}$ appear to be much stronger than in $\text{LaFeAsO}_x\text{F}_{1-x}$. The effect of thermal fluctuations is quantified by the Ginzburg parameter, $Gi = (2k_B T_c / \phi_0^2) (\lambda_0^2 / \xi_c^2) = 2$, $\xi_c = \lambda_0 \frac{1}{\gamma}$ is the coherence length along the c -axis, $\gamma = m_c/m_a$ is the mass anisotropy parameter in a uniaxial crystal [32].

For $\text{LaFeAsO}_x\text{F}_{1-x}$, ξ_c can be estimated from the zero temperature $H_{c2}^k(0) = \phi_0 / 2 \lambda_0 \gamma$, which yields $\xi_c = [\phi_0 / 2 H_{c2}^k(0)]^{1/2} = 1.2$ nm for $\gamma = 15$ [3] and $H_{c2}^k(0) = 60$ T [16]. In this case $Gi = 3.4 \times 10^4$ is only 50% higher than $Gi = 2.1 \times 10^4$ of clean MgB_2 ($T_c = 40$ K, $\lambda_a = 5$ nm, $\gamma = 36$, and $\lambda_c = \lambda_a \gamma = 25$ [34]), but some 30 times smaller than Gi for the least anisotropic cuprate, $\text{YBa}_2\text{Cu}_3\text{O}_{7-x}$ [32]. Since ξ_c is inversely proportional to T_c , the slope $dH_{c2}^k/dT = T_c^{-1/2}$ near T_c in the clean limit increases as T_c and γ increase. The values of dH_{c2}^k/dT estimated from the slopes of $H_{90}(T)$ in Fig. 3 increase from 2.7 T/K for $\text{LaFeAsO}_x\text{F}_{1-x}$ to 9.3 T/K for SmFeAsO , indicating that SmFeAsO is more anisotropic with $\gamma = 15(9.3/2.7)^2 = 65$,

which exceeds the anisotropy parameter 25 50 of YBCO. This estimate is very close to 64 at T_c inferred from the recent torque magnetic measurements on $\text{SmFeAs}(\text{O},\text{F})$ single crystals, which also revealed a temperature dependence of $\xi(T)$ indicative of two-band superconductivity [35]. The impact of high anisotropy on the Ginzburg parameter for SmFeAsO is large: $G i^{\text{Sm}} = G i^{\text{La}} = (T_c^{\text{Sm}} / T_c^{\text{La}})^4 (c_{\text{Sm}} / c_{\text{La}})^2$, 35 and $G i^{\text{Sm}}$ is thus of the same order as $G i$ for YBCO. Our conclusions are also consistent with the recent measurements of H_{c2} on $\text{NdFeAs}(\text{O},\text{F})$ single crystals, for which $dH_{c2}^k/dT = 9 \text{ T/K}$, $dH_{c2}^2/dT = 1.85 \text{ T/K}$, $a = 1.85 \text{ nm}$, $c = 0.38 \text{ nm}$, and $\xi = 20 - 40$ depending on the sample purity [36]. These values of ξ are close to those for YBCO. Moreover, taking $\xi_0 = 200 \text{ nm}$, $c = 0.38 \text{ nm}$ and $T_c = 49 \text{ K}$, we again obtain $G i \sim 10^2$, a typical Ginzburg number for YBCO. For two-band superconductors, the above estimates of $G i$ remain qualitatively the same if ξ_0 and c are taken for the band with the minimum effective mass or maximum electron mobility [31].

The relatively small value of $G i$ in the La compound indicates that the melting field of the vortex lattice, $H_m(T)$ is not too different from H_{c2} [16]. However, for Sm and Nd compounds, the difference between H_m and H_{c2} becomes more pronounced because of the much larger Ginzburg numbers. In this case $H_m \ll H_{c2}$, even for a moderately anisotropic superconductor, for which

$$H_m = a H_{c2}(0) \frac{T_c^2}{T^2} \left(1 - \frac{T}{T_c} \right)^2 : \quad (2)$$

Here $a = \xi_0^4 / c_L^4 = G i$, and $c_L = 0.17$ is the Lindemann number for the vortex lattice [32]. Taking the above-estimated value of $G i \sim 1.3 \times 10^2$ for SmFeAsO , we obtain $a \sim 0.63$. Here the melting field $H_m(T)$ exhibits an upward curvature near T_c where $H_m(T)$ is significantly smaller than $H_{c2}(T) = H_{c2}(0)(1 - T/T_c)$. At lower temperatures $H_m(T)$ crosses over with $H_{c2}(T)$ in the same way as in cuprates [32].

In conclusion, we have measured magneto-transport in three of the rare earth oxypnictide superconductors: $\text{LaFeAsO}_{0.89}\text{F}_{0.11}$, $\text{SmFeAsO}_{0.85}$, and $\text{NdFeAsO}_{0.94}\text{F}_{0.06}$. From resistivity, Hall coefficient and upper critical magnetic fields, we conclude that $\text{LaFeAsO}_{0.89}\text{F}_{0.11}$ behaves as an intermediate- T_c superconductor like MgB_2 in which thermal fluctuations of vortices do not significantly affect the $H-T$ diagram to the extent that they do in the layered cuprates. However, the situation is different for the higher- T_c oxypnictides, SmFeAsO and $\text{NdFeAs}(\text{O},\text{F})$, which exhibit a larger mass anisotropy, enhanced thermal fluctuations, and for which the Ginzburg parameter becomes comparable to that of YBCO. Thus, the series of oxypnictide superconductors bridges a conceptual gap between conventional superconductors and the high-temperature cuprates. As such, they hold particular promise for understanding the many still-unexplained

behaviors of the high- T_c cuprates.

The work at NHMFL was supported by the NSF Cooperative Agreement No. DMR-0084173, by the State of Florida, by the DOE, by the NHMFL IHRP program (FH), and by AFOSR grant FA9550-06-1-0474 (AG and DCL). Work at ORNL was supported by the Division of Materials Science and Engineering, Office of Basic Energy Sciences.

-
- [1] Y. Kamihara, T. Watanabe, M. Hirano, and H. Hosono. Iron-Based Layered Superconductor $\text{LaO}_{1-x}\text{F}_x\text{FeAs}$ ($x = 0.05 - 0.12$) with $T_c = 26 \text{ K}$. *J. Am. Chem. Soc.* 130, 3296 (2008).
 - [2] H. Takahashi, K. Igawa, K. Arii, Y. Kamihara, M. Hirano, and H. Hosono. Superconductivity at 43 K in an iron-based layered compound $\text{LaO}_{1-x}\text{F}_x\text{FeAs}$. *Nature* 453, 376 (2008).
 - [3] A. S. Sefat, M. A. McGuire, B. C. Sales, R. Jin, J. Y. Howe, and D. Mandrus. Electronic correlations in the superconductor $\text{LaFeAsO}_{0.89}\text{F}_{0.11}$ with low carrier density. *Phys. Rev. B* 77, 174503 (pages 6) (2008).
 - [4] G. F. Chen, Z. Li, D. Wu, G. Li, W. Z. Hu, J. Dong, P. Zheng, J. L. Luo, and N. L. Wang. Superconductivity at 41 K and its competition with spin-density-wave instability in layered $\text{CeO}_{1-x}\text{F}_x\text{FeAs}$. *Phys. Rev. Lett.* 100, 247002 (2008).
 - [5] Z.-A. Ren, J. Yang, W. Lu, W. Yi, X.-L. Shen, Z.-C. Li, G.-C. Che, X.-L. Dong, L.-L. Sun, F. Zhou, et al. Superconductivity in iron-based F-doped layered quaternary compound $\text{NdO}_{1-x}\text{F}_x\text{FeAs}$. *Europhysics Letters* 82, 57002 (2008).
 - [6] Z.-A. Ren, J. Yang, W. Lu, W. Yi, G.-C. Che, X.-L. Dong, L.-L. Sun, and Z.-X. Zhao. Superconductivity at 52 K in iron-based F-doped layered quaternary compound $\text{PrO}_{1-x}\text{F}_x\text{FeAs}$ (2008), [arXiv.org/0803.4283](http://arxiv.org/0803.4283), unpublished.
 - [7] X. H. Chen, T. Wu, G. Wu, R. H. Liu, H. Chen, and D. F. Fang. Superconductivity at 43 K in samarium-arsenide oxides $\text{SmFeAsO}_{1-x}\text{F}_x$ (2008), [arXiv.org/0803.3603](http://arxiv.org/0803.3603), unpublished.
 - [8] J. Yang, Z.-C. Li, W. Lu, W. Yi, X.-L. Shen, Z.-A. Ren, G.-C. Che, X.-L. Dong, L.-L. Sun, F. Zhou, et al. Superconductivity at 53.5 K in $\text{GdFeAsO}_{1-x}\text{F}_x$. *Superconductor Science and Technology* 21, 082001 (2008).
 - [9] Z.-A. Ren, W. Lu, J. Yang, W. Yi, X.-L. Shen, Z.-C. Li, G.-C. Che, X.-L. Dong, L.-L. Sun, F. Zhou, et al. Superconductivity at 55 K in iron-based F-doped layered quaternary compound $\text{SmO}_{1-x}\text{F}_x\text{FeAs}$. *Chin. Phys. Lett.* 25, 2215 (2008).
 - [10] A. Yamamoto, A. Polyanskii, J. Jiang, F. Kametani, C. Tarantini, F. Hunte, J. Jaroszynski, E. Hellstrom, P. Lee, A. Gurevich, et al. Evidence for two distinct scales of current flow in polycrystalline Sm and Nd iron oxypnictides. *Superconductor Science and Technology* 21, 095008 (2008).
 - [11] A. Yamamoto, J. Jiang, C. Tarantini, N. Craig, A. A. Polyanskii, F. Kametani, F. Hunte, J. Jaroszynski, E. E. Hellstrom, D. C. Larbalestier, et al. Evidence for electronic granularities in the polycrystalline iron-based

- superconductor $\text{LaO}_{0.89}\text{F}_{0.11}\text{FeAs}$. *Applied Physics Letters* 92, 252501 (2008).
- [12] T. Fujitake (2008), to be published.
- [13] R. H. Liu, G. Wu, T. Wu, D. F. Fang, H. Chen, S. Y. Li, K. Liu, Y. L. Xie, X. F. Wang, R. L. Yang, et al. Phase Diagram and Quantum Critical Point in Newly Discovered Superconductors: $\text{SmO}_{1-x}\text{F}_x\text{FeAs}$ (2008), [arXiv.org:0804.2105](https://arxiv.org/abs/0804.2105), unpublished.
- [14] G. F. Chen, Z. Li, D. Wu, J. Dong, G. Li, W. Z. Hu, P. Zheng, J. L. Luo, and N. L. Wang. Element substitution effect in transition metal oxypnictide $\text{Re}(\text{O}_{1-x}\text{F}_x)\text{TAs}$ (Re = rare earth, T = transition metal). *Chinese Physics Letters* 25, 2235 (2008).
- [15] G. Giovannetti, S. Kumar, and J. van den Brink. Mot State and Quantum Critical Points in Rare-Earth Oxypnictides $\text{RO}_{1-x}\text{F}_x\text{FeAs}$ (R = La, Sm, Nd, Pr, Ce) (2008), [arXiv.org:0804.0866](https://arxiv.org/abs/0804.0866), unpublished, *Phys. Rev. B*, in press.
- [16] F. Hunte, J. Jaroszynski, A. Gurevich, D. C. Larbalestier, R. Jin, A. S. Sefat, M. A. McGuire, B. C. Sales, D. K. Christen, and D. Mandrus. Two-band superconductivity in $\text{LaFeAsO}_{0.89}\text{F}_{0.11}$ at very high magnetic fields. *Nature* 453, 903 (2008).
- [17] Y. Wang, L. Shan, L. Fang, P. Cheng, C. Ren, and H. H. Wen. Nodal superconductivity with multiple gaps in $\text{sm-feaso}_{0.9}\text{f}_{0.1}$ (2008), [arXiv.org:0806.1986](https://arxiv.org/abs/0806.1986), unpublished.
- [18] K. Matano, Z. A. Ren, X. L. Dong, L. L. Sun, Z. X. Zhao, and G. Qing Zheng. Spin-singlet superconductivity with multiple gaps in $\text{pr}_{0.89}\text{f}_{0.11}\text{feas}$ (2008), [arXiv.org:0806.0249](https://arxiv.org/abs/0806.0249), unpublished.
- [19] F. Ma and Z.-Y. Lu, Iron-based layered superconductor $\text{LaO}_{1-x}\text{F}_x\text{FeAs}$: an antiferromagnetic semimetal (2008), [arXiv.org:0803.3286](https://arxiv.org/abs/0803.3286).
- [20] S. Raghu, X.-L. Qi, C.-X. Liu, D. J. Scalapino, and S.-C. Zhang. Minimal two-band model of the superconducting iron oxypnictides. *Physical Review B* 77, 220503 (2008).
- [21] Q. Han, Y. Chen, and Z. D. Wang. A generic two-band model for unconventional superconductivity and spin-density-wave order in electron- and hole-doped iron-based superconductors. *EPL (Europhysics Letters)* 82, 37007 (2008).
- [22] C. Kittel, *Introduction to Solid State Physics* (Wiley, John & Sons, New York, 2004).
- [23] C. de la Cruz, Q. Huang, J. W. Lynn, J. Li, W. Ratcliff II, J. L. Zarestky, H. A. Mook, G. F. Chen, J. L. Luo, N. L. Wang, et al. Magnetic Order versus superconductivity in the Iron-based layered $\text{La}(\text{O}_{1-x}\text{F}_x)\text{FeAs}$ systems. *Nature* 453, 899 (2008).
- [24] C. W. Jee and H. Zhou (2008), unpublished.
- [25] M. Frattini, R. Caivano, A. Puri, A. Ricci, Z.-A. Ren, X.-L. Dong, J. Yang, W. Lu, Z.-X. Zhao, L. Barba, et al. The effect of internal pressure on the tetragonal to monoclinic structural phase transition in ReOFeAs : the case of NdOFeAs (2008), [arXiv.org:0805.3992](https://arxiv.org/abs/0805.3992), unpublished.
- [26] Y. Ando, G. S. Boebinger, A. Passner, L. F. Schneemeyer, T. Kimura, M. Okuya, S. Watauchi, J. Shimoyama, K. Kishio, K. Tamasaku, et al. Resistive upper critical fields and irreversibility lines of optimally doped high- T_c cuprates. *Phys. Rev. B* 60, 12475 (1999).
- [27] K. Ahilan, F. L. Ning, T. Imai, A. S. Sefat, R. Jin, M. McGuire, B. Sales, and D. Mandrus. ^{19}F NMR Investigation of $\text{LaAsFeO}(0.89)\text{F}(0.11)$ Superconductor (2008), [arXiv.org:0804.4026v1](https://arxiv.org/abs/0804.4026v1), unpublished.
- [28] H. Luetkens, H. H. Klauss, R. Khasanov, A. Amato, R. Klingeler, I. Hellmann, N. Leps, A. Kondrat, C. Hess, A. Kohler, et al. Field and temperature dependence of the superfluid density in $\text{LaO}_{1-x}\text{F}_x\text{FeAs}$ superconductors: A muon spin relaxation study (2008), [arXiv.org:0804.3115](https://arxiv.org/abs/0804.3115), unpublished.
- [29] A. J. Drew, F. L. Pratt, T. Lancaster, S. J. Blundell, P. J. Baker, R. H. Liu, G. Wu, X. H. Chen, I. Watanabe, V. K. Malik, et al. Coexistence of magnetism and superconductivity in the pnictide high temperature superconductor $\text{SmO}_{0.82}\text{F}_{0.18}\text{FeAs}$ measured by muon spin rotation (2008), [arXiv.org:0805.1042](https://arxiv.org/abs/0805.1042), unpublished.
- [30] I. I. Mazin, D. J. Singh, M. D. Johannes, and M. H. Du. Unconventional sign-reversing superconductivity in $\text{LaFeAsO}_{1-x}\text{F}_x$ (2008), [arXiv.org:0803.2740](https://arxiv.org/abs/0803.2740), unpublished.
- [31] A. Gurevich. Limits of the upper critical field in dirty two-gap superconductors. *Physica C* 456, 160 (2007), Enhancement of the upper critical field by nonmagnetic impurities in dirty two-gap superconductors, *Phys. Rev. B* 67, 184515 (2003).
- [32] G. B. Latter, M. V. Feigel'man, V. B. Geshkenbein, A. I. Larkin, and V. M. Vinokur. Vortices in high-temperature superconductors. *Rev. Mod. Phys.* 66, 1125 (1994).
- [33] D. J. Singh and M. H. Du. $\text{LaFeAsO}_{1-x}\text{F}_x$: A low carrier density superconductor near itinerant magnetism. *Phys. Rev. Lett.* 100 (2008).
- [34] P. Canfield, S. Bud'ko, and D. Finnemore. An overview of the basic physical properties of MgB_2 . *Physica C* 385, 1 (2003).
- [35] S. Weyeneth, U. Mosele, N. Zhigadlo, S. Katrych, Z. Bukowski, J. Karpinski, S. Kohout, J. Roos, and H. Keller. Magnetic anisotropy of single crystal $\text{SmO}_{0.8}\text{F}_{0.2}\text{FeAs}$ studied by torque magnetometry (2008), [arXiv.org:0806.1024](https://arxiv.org/abs/0806.1024), unpublished.
- [36] Y. Jia, Y. Cheng, L. Fang, H. Luo, H. Yang, C. Ren, L. Shan, and H. Wen. Critical fields and anisotropy of $\text{NdO}_{0.82}\text{F}_{0.18}\text{FeAs}$ single crystal (2008), [arXiv.org:0806.0532](https://arxiv.org/abs/0806.0532), unpublished.